COBEM 2015

ABCM Associação Brasileira de Engenharia e Ciências Mecânicas

23rd ABCM International Congress of Mechanical Engineering
December 6-11, 2015, Rio de Janeiro, RJ, Brazil

DESIGN OF A DESCRIPTOR FOR ALIGNING SURFACE RANGE IMAGES WITH APPLICATION TO ROBOTICS

Gerardo Antonio Idrobo Pizo
José Mauricio Santos Torres Motta
Universidade de Brasília, Departamento de Engenharia Mecânica,
Grupo de Automática e Controle (GRACO),
CEP 70910-900, Brasília, DF.
gerardo.idrobo@gmail.com ; jmmotta@unb.br

Abstract. *The 3D reconstruction of objects from range images comprises three steps: a) acquisition, in which the object surface is scanned from various viewpoints, generating a set of n range images; b) registration, in which a rigid transformation M must be estimated to position images, peer to peer, in a single frame and c) matching, in which redundancies between registered views are treated to build a single and complete 3D model. This work proposes a methodology to register range images based on segmentation/reconstruction making use of an edge detection technique combined with a clustering technique using mesh decimation. The descriptor is applied to contours and it is invariant to similarity transformations including rotation, translation and uniform scale and also robust to noise. The proposed descriptor makes use of n corresponding points extracted from two images and a signature label is assigned specifically to a point considering the geometrical distribution of its neighborhood, facilitating the identification of possible areas of overlapping and reducing the ambiguity in the search process. The descriptor was evaluated through a series of tests with various object range images. To verify the validity of the candidate transformations, each of which passes through a fine alignment and the fitting errors between the two range images are evaluated by the ICP algorithm. The transformation that aligns the largest number of points is considered the solution.*

Keywords: *Image Registration, Range Imaging, Image Descriptors, 3D Surface Reconstruction, ISO GUM.*

1. INTRODUCTION

The purpose of this work is to contribute to a strategy for the registration of range images aiming at constructing 3D surface maps for robotics. The classic paradigm for estimating the rigid similarity transformation between two range images is to minimize the distance error between pairs of corresponding points extracted from both images. Therefore, the main task of the registration process is the automatic determination of the corresponding pairs of feature points between views that can be translated, rotated and/or scaled relative to each other. The solution of this problem becomes a challenge, since the correspondence between the overlapping regions from which the pairs of corresponding points are to be extracted is unknown.

Besl (1992) proposed the iterative ICP (Iterative Closest Point) algorithm, stating that the closest points between two images are the corresponding points. To find such correspondences the algorithm requires an initial transformation ($\boldsymbol{T}_0$) that approximates sufficiently both images. In this way, a need arises for a previous rough alignment of the range images. Planitz (2005) presented some techniques to resolve this issue in two approaches: in the first, the matches are obtained from the full set of the original samples; in the second, the matches are obtained from a subset of the original data, consisting of samples that have special features. These techniques, however, still have certain limitations. In the first case, the search space is too large, making the technique inefficient. In the second case, some important information for the matching process can be lost for being restricted only to a specific set of data. In this paper it is proposed a rough alignment algorithm that circumvents these limitations based on two innovations. It is proposed that instead of using the full set of samples from an image, it is used a simplified triangular mesh constructed with the technique of deformable models (Chui et al., 2008). This allows that global features of the original image are preserved and the corresponding pairs are obtained from small spaces composed by the control points of the mesh (corners). In addition, it is proposed a methodology that combines multiple descriptors by using a general descriptor, making correspondences in between the small spaces of the samples possible. Unlike the existing proposals, this one integrates local and global geometric sample information, making it to be more discriminating in the search process.

The technique of rough alignment proposed was integrated with a fine alignment technique, establishing a complete methodology for registration and reconstruction of 3-D surface models. Apart from that, it is very important to evaluate the registration process as a function of the location of the corresponding points. The measurement uncertainty is a robust indicator of the quality of this process, since it takes into account the potential significant sources of error. The Guide to the expression of Uncertainty in Measurement (GUM ISO) provides guidelines for the evaluation of uncertainty of the registration process.

2. ROUGH ALIGNMENT OF RANGE IMAGES

Several steps of the rough alignment method proposed are shown in Fig. 1.

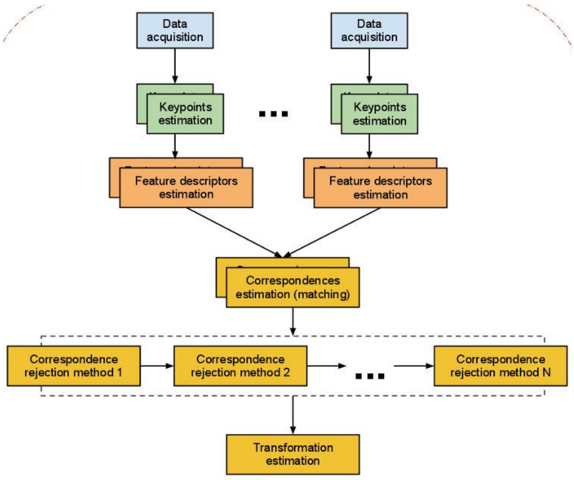

Figure 1. Block Diagram showing the main steps for the rough alignment of range images

The process starts with the acquisition of point clouds followed by data reduction and image segmentation for extracting contour curves. Any curve $C(u)$ can be represented in discrete form by an ordered sequence of straight line segments that connect points. Some of these points stand out over others by representing specific regions, and can be used in the correspondence estimation process between two images.

Next, a step for sorting feature points accepting or rejecting them is carried out by checking the compatibility between the feature points and their neighborhood, when the points are within a corresponding area of pre-alignment.

In the next section the steps of the methodology for the rough alignment are described. The steps will be discussed with experimental results for a better understanding of the procedures adopted.

2.1. Step 1: Clouds of Points

As a test procedure, three range images of a metallic object model characterizing the face of a horse were acquired. The three range images were: (a) a reference image of the complete object (Fig. 2a) and (b) two other range images, $\boldsymbol{I}_1$and $\boldsymbol{I}_2$ **,** of a partial view of the object (Fig. 2b), but sharing an overlap area σ_s of approximately 40%.

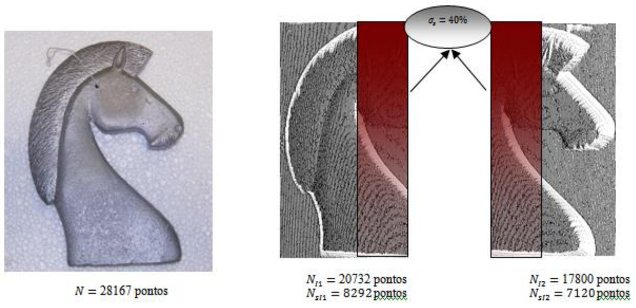

(a) image of the complete object

(b) Range image (I_1 (left) , I_2(right))

Table 1. Image properties - number of points

$N = 28167$points	Number of points of the range image of the complete object;
$N_{I1} = 20732$ points	Number of points of the range image $\mathbf{I_1}$;
$N_{sI1} = 8292$ points	Number of points of the range image $\mathbf{I_1}$ overlapped on the second range image;
$N_{I2} = 17800$ points	Number of points of the range image $\mathbf{I_2}$;
$N_{sI2} = 7120$ points	Number of points of the range image $\mathbf{I_2}$ overlapped on the first range image;

Figure 2. Range images acquired with the scanner VISCAN3D (Ginani, 2008).

2.2. Step 2: Data reduction

The range images acquired result in hundreds of samples, making efficient data processing a challenging task. In fact, the main issue to increase efficiency of the rough alignment procedures is the reduction of the domain space of the descriptors in the range image $\boldsymbol{I}_1$, and also in the search space of the corresponding descriptors in the range image $\boldsymbol{I}_2$. This reduction is viable by decreasing the amount of data in the range images, replacing the dense set of samples by a smaller set that captures the essence of the original surface profile. In this work, the range image $\boldsymbol{I}_1$ has its samples organized by a mesh deformation process when the point cloud is projected on the surface (Fig. 3). According to tests carried out and presented in the dissertation of Idrobo Pizo (2009) it can be proved that this approach can reduce the amount of data by up to 90%, guaranteeing efficiency and resulting in a density enough to that preserve the existence of properties after proper adjustments of the control parameters.

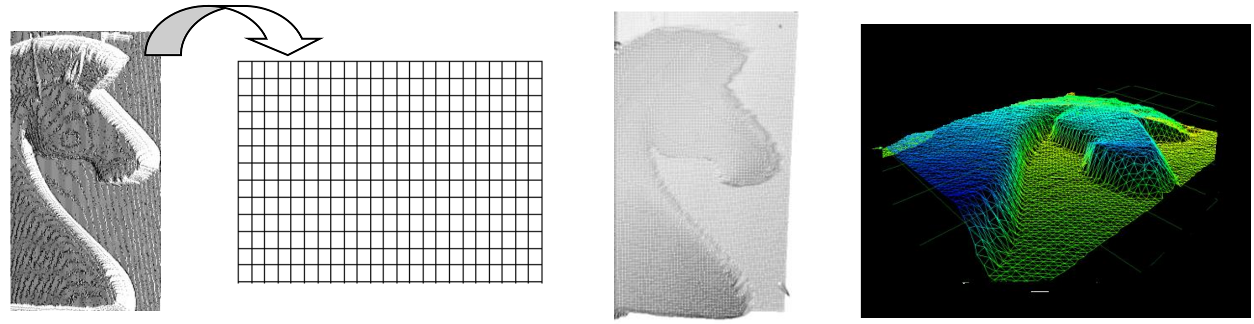

(a) Cloud of Points (b) Projection of a cloud of points on a structured mesh (c) 2D triangular mesh. (d) 3D triangular mesh.

Figure 3. Procedures for data reduction

Table. 2. Statistics of the reduced data.

Range Image	Points	Remaining points after data reduction	% preservation of the original range image
I_1-Horse	20732	5256	~26
I_2-Horse	17800	3978	~22

2.3. Step 3:Labeling of Regions

The detection of the contour curves can be achieved from the values of the depth variation between the cloud points and their neighbors. Experimentally, the curves are extracted from a histogram of the points satisfying certain conditions. The histograms described in Fig. 4a show the frequency of points whose angle of orientation (γ) of the normal vector to the surface, at the points belonging to the range images I_1 and I_2 respectively, have values between [0 - 1] and are associated to depths of at least 50% of the depth of the deepest point on the edge.

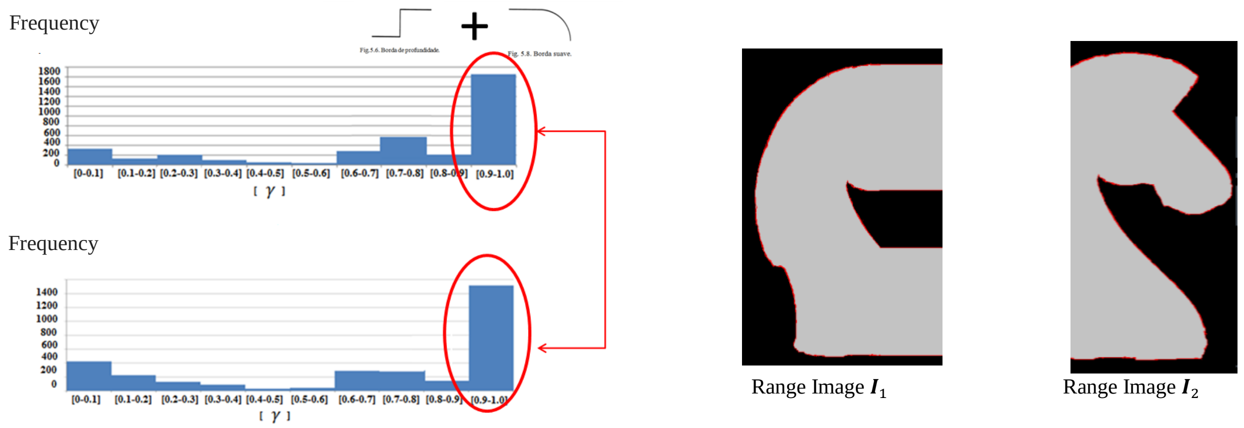

(a) Histogram of the range images $\mathbf{I_1}$ **e** $\mathbf{I_2}$

(b) Refinement of the segmented range image – contour map construction.

Figure 4. Map Segmentation

Surface Normal Vector
$$\vec{n}(u,v) = \frac{(-f_u, -f_v, 1)^T}{\sqrt{(1 + {f_u}^2 + {f_v}^2)}}$$

Orientation Angle of the Normal Vector
$$\gamma(u,v) = \cos\left(tan^{-1}\left(\frac{f_u}{f_v}\right)\right) \quad (1)$$

where

- f (u, v) is the depth value at the coordinate (u, v) of a point on the surface;
- f_u = partial derivative of f (u, v) with respect to u;
- f_v = partial derivative of f (u, v) with respect v;

Concerning the example discussed, the orientation angle γ (Eq. (1)) of the contour curves takes values in the range of γ = [0.9 to 1.0], such that all the other values define the image ground. These parameters were chosen aiming at selecting large contours of continuous regions with high noise attenuation. With other γ values the image contours detected may present noise that disrupts the areas segmented. In Fig. 4b, experimental results illustrate the applicability of the proposed method to image segmentation for constructing 3D depth maps. The images shown highlight the clear identification of the object borders (red line). The information that the contour curves contain will be used to determine the correspondence between two surface point clouds that have to be aligned.

2.4. Step 4: Detection of Feature Points on Contour Curves

Any open or closed continuous curve can be represented as a discrete curve C(u) that can be represented by an ordered sequence of straight line segments that connect two points, such that $C_u = u_1 u_2 \ldots u_n,$, where $\{u_i: 1 \leq i \leq n\}$ and n indicates the number of points of the curve, and u_i can be labeled by eight states. The states associated with each element u_i represent the relative direction between two feature points along the curve, approximated to one of the multiple directions of 45 degrees (Fig. 5a).

The chain code (Freeman and Davis, 1977) is generated at the same time as following the curve elements. Figure (5.b) provides an example of the assignment of states to a curve. The process starts on the shaded end.

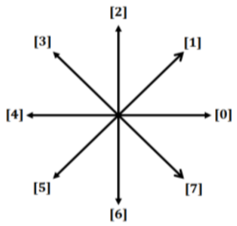

(a) 8-state directional code.

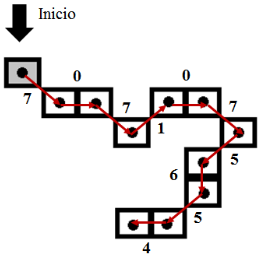

(b). Example of chain code (c.8) 7071075654.

Figure 5. chain code

In the case of closed curves, the chain code finishes when the curve trace returns to the starting point. The encoding described is absolute, in the sense that each state represents a constant direction with reference to the initial point. According to Gonzales (2008) the method presents several limitations: (1) the resulting code is too long; (2) any small disturbance along the curve due to noise or imperfect segmentation causes variations in the code that may not be necessarily related to the curve shape; (3) the chain code depends on the chosen starting point (in the case of open curves there is ambiguity concerning the start end).

2.4.1. Optimization of the Chain Code Algorithm for Finding Feature Points

In this section a new algorithm to avoid the limitations of the chain code is described. First, it is presented the steps of the proposed algorithm to filter out noise and to determine feature points, and next each feature point is marked by a signature related to its neighbor point. The signature assigned to each point is invariant to similarity transformations. The descriptor is based on operations with integers, which brings about benefits by being simple to program in any type of hardware (microcontrollers, FPGAs, microprocessors, among others) and it is computationally efficient.

The steps of the proposed algorithm to label feature points of a curve are described following:

Step [1]. Smooth the curve C(u) attenuating noise by using the NLMS Adaptive Filter:

A curve ($\boldsymbol{C}_u$) of a point cloud can be modeled as an ordered sequence of $\boldsymbol{u}_n$ straight line segments that connect two points and can be represented as $\boldsymbol{C}_u = \boldsymbol{H}_u \boldsymbol{u}_n + \boldsymbol{v}_u$, in which $\boldsymbol{H}_u$is the observation model that transforms the real state space into the observation space and $\boldsymbol{v}_u$ is the observation noise considered as a Gaussian white noise with zero mean.

Figure 6a shows a diagram representing graphically the noise attenuation algorithm. The process wraps the desired output signal of the filter $\boldsymbol{G}_u = \boldsymbol{V}_u \boldsymbol{u}_n$ and the error estimation by comparing the desired signal and the input signal $\boldsymbol{e_u} = \boldsymbol{C}_u - \boldsymbol{G}_u = (\boldsymbol{H}_u - \boldsymbol{V}_u)\boldsymbol{u}_n + \boldsymbol{v}_u$. An ideal case of noise filtering would be $\boldsymbol{H}_u = \boldsymbol{V}_u$, therefore yielding $\boldsymbol{e_u} = \boldsymbol{v}_u$. Thus, the noise would be completely identified and eliminated. However, the approximation of $\boldsymbol{V}_u$ to $\boldsymbol{H}_u$ by a filter of finite length and precision impedes noise to be perfectly modeled.

The $\boldsymbol{V}_u$ operator is obtained iteratively by the NLMS algorithm, which can be expressed by the following equation:

$$\boldsymbol{V}_u = \boldsymbol{V}_{u-1} + \frac{\mu_{NLMS}\, \boldsymbol{e}_u \boldsymbol{u}_n}{\boldsymbol{u}_n^T \boldsymbol{u}_n}, \tag{2}$$

where μ (NLMS) is the performance parameter value, with values in the range [0 - 1].

Figure 6b shows the input signal to the NLMS filter. Figure 6b show the output signal of the NLMS filter for different values of the performance parameter. As the value of μ_{NLMS} is decreased the $\boldsymbol{G_u}$ curve gets smoother compared to the $\boldsymbol{C_u}$curve.

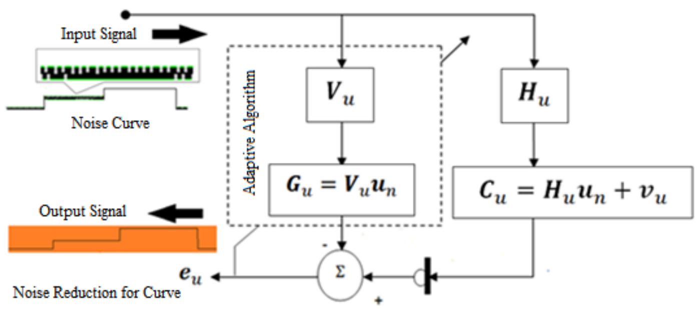

(a). Diagram showing the noise attenuation process for a curve.

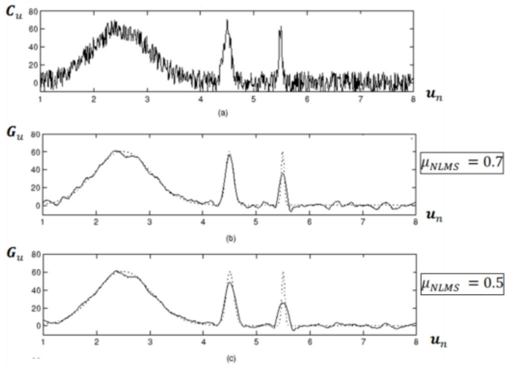

(b) Noise attenuation for different performance parameters. The dotted line is the original points before using the performance parameter on the curve $\boldsymbol{C_u}$.

Figure 6. Adaptive Filter NLMS

Step [2]. Represent the u_n segments of the curve in a graph *state vs segments* (Fig. 7a).

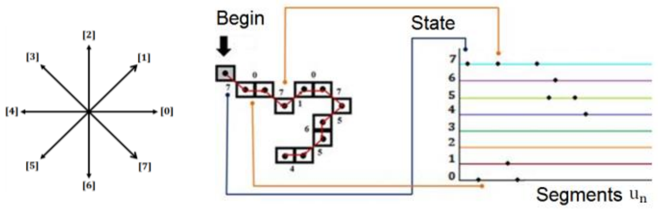

8-state directional code

$C(u) = u_1 u_2 \ldots u_n$

Graphic *state vs segments*

(a) Data Representation *state vs segments.*

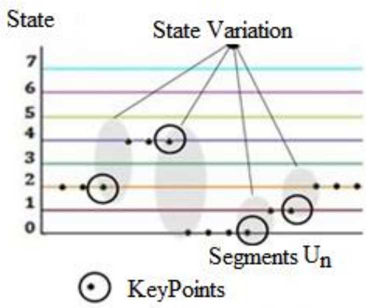

(b) Detection of feature points in the graphic *state vs segments*

Figure 7. Detection of feature points

Step [3]. Calculate the change in direction of the segments by using the angle $\alpha(u_n)$ between points (Eq. (3)). The general strategy to build the descriptor is not to determine local points, but the values defined by the points that measure the change in state (Fig. 7b).

$$\alpha(u_n) = abs\left[tan^{-1}(\frac{u_{n+1}}{u_n})\right] \tag{3}$$

A feature point is detected if $\alpha(u_n) \neq 0$.

Step [4]. Identify the feature points on the curve $C(u)$ that were detected in the graphic *state vs. segments*. Connect the feature points by straight line segments $\vec{v}_m$ (Fig 8a and Fig. 8b);

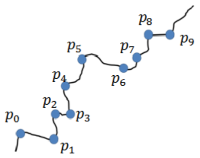

(a) Identified feature points on a curve.

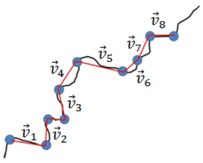

(b) Feature points linked forming segments.

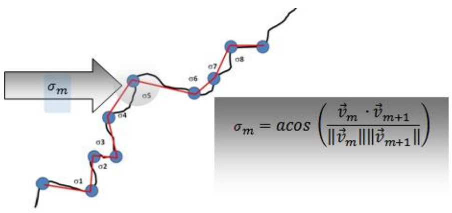

(c) Calculation of the angle between segments connecting feature points.

Figure 8. Identified feature points on a curve and Calculation of the angle between segments connecting

Step [5]. Calculate the change in direction of the segments (angle σ_m) between $\vec{v}_m$ and $\vec{v}_{m+1}$ by the scalar product (Fig. 8c).

Step [6]. Discretize the angles σ_m in 4 directional code states (Tab. 3) and perform a graphical representation of the discrete angle $(\sigma_d)_{4E}$[1] through the barcode. For a better display one can assign one color for each state.

Figure 9. Detection of the feature points over a barcode.

Table 3. Discrete values associated to the 4-state directional codes.

Angle variation(σ_m)	Discrete Angle$(\sigma_d)_{4E}$	Representative color
$\sigma_m < 45°$	$\sigma_d = 0$	
$45° \leq \sigma_m < 90°$	$\sigma_d = 1$	
$90° \leq \sigma_m < 135°$	$\sigma_d = 2$	
$135° \leq \sigma_m < 180°$	$\sigma_d = 3$	

For the particular case of the previous example there is a single point in the barcode that stands out among the others (Fig. 9). The point belongs to the zero state (yellow color) and it is indicated by an arrow. This particular feature point can be the seed point to perform a quick rough alignment between images. The same process can happen for any number of curves. The points selected as corresponding points must take a numeric code that identifies the region to which it belongs. This code was named, in this work, the signature feature point.

Step [7]. For generating the signature, the information is collected from the neighborhood connecting the feature point PP to its six closest neighbors. The process can be seen graphically in Figure 10.

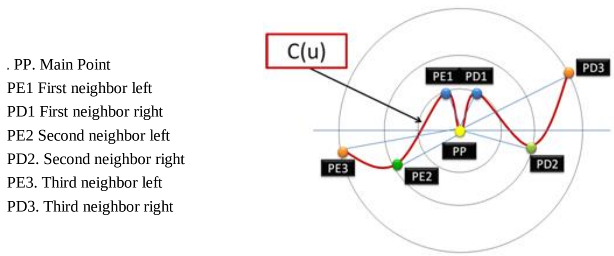

Figure 10. Process to generate the signature associated to a feature point.

Step [8]. The variation of the directions of the segments is calculated from the scalar products that can be estimated successively, as shown in the Tab. 4.

Table 4. Data colected from the angles between segments of feature points for the generation a signature – curve $\boldsymbol{C(u)}$.

	Angles between segments				
	PE1PPPD1	PE1PPPE2	PE2PPPE3	PD1PPPD2	PD2PPPD3
(σ_m)	Main Angle ~33°	~98°	~18°	~87°	~52°

Table 5. Data organized from the angles between feature points for the generation a signature – curve $\boldsymbol{C(u)}$.

	Angles between segments				
	PE1PPPD1	PE2PPPE3	PD2PPPD3	PD1PPPD2	PE1PPPE2
(σ_m)	Main Angle ~33°	~18°	~52°	~87°	~98°

Step [9]. The angle values are ordered ascendingly. The ordering of the angles starts from the main angle. Ordering the angles allows the descriptor proposed to be invariant to rotations (Tab. 5);

[1] $(\sigma_d)_{4E} \rightarrow$ symbol for an angle discretized by a 4-state directional code (4E)

Step [10]. Discretize the angles σ_m making use of the values of the 4-state directional code (Tab. 6). Then, there is a full signature as a numeric code by ordering the discretized digit angles (σ_d), (Tab. 7).

Table 6. Discrete values assigned to the angle variation $(\boldsymbol{\sigma_m})$by the 4-state directional code.

Angle Variation(σ_m)	Discrete Angle $(\sigma_d)_{4E}$
$\sigma_m < 45°$	$\sigma_d = 0$
$45° \leq \sigma_m < 90°$	$\sigma_d = 1$
$90° \leq \sigma_m < 135°$	$\sigma_d = 2$
$135° \leq \sigma_m < 180°$	$\sigma_d = 3$

Table 7. Discrete angles making use of the 4-state directional code – full signature.

	Angle between point segments				
	PE1PPPD1	PE2PPPE3	PD2PPPD3	PD1PPPD2	PE1PPPE2
(σ_m)	Principal Angle ~33°	~18°	~52°	~87°	~98°
$(\sigma_d)_{4E}$	0 1° Digit	0 2° Digit	1 3° Digit	1 4° Digit	2 5° Digit
Full Signature PP	0 1° Digit	0 2° Digit	1 3° Digit	1 4° Digit	2 5° Digit

During the curve $C(u)$ characterization process the optimization algorithm does not prevent that there are closed curves. To avoid this a step further can be included.

Step [11]. When the start and end points are equal, the algorithm terminates.

The proposed descriptor extracts feature points of a curve that are labeled in such a way that it is invariant to any geometric similarity transformation. The algorithm reduces the limitations of the original chain code algorithm.

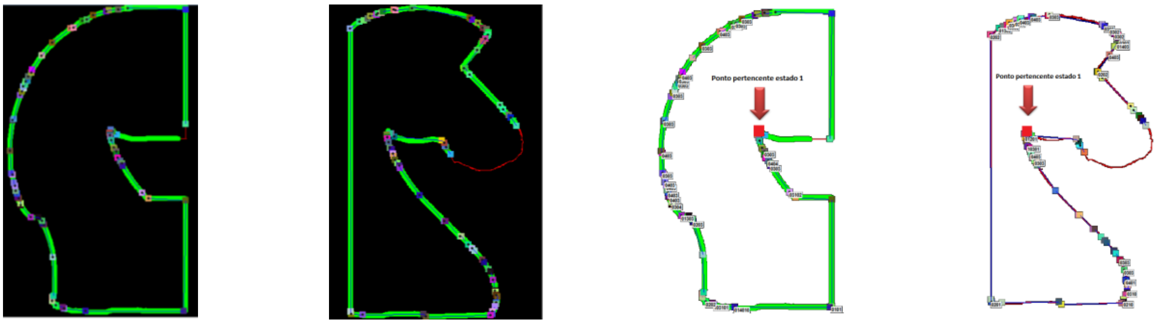

(a) Identification of points I_1 (b) Identification of points I_2 (c) Signature of points $\boldsymbol{I_1}$ (d) Signature of points $\boldsymbol{I_2}$

Figure 11. Detection of feature points with their corresponding signatures

2.4.2. Detection of Contour Curves: Experimental Results

In this section it is presented the experimental results of the algorithm to detect of feature points from the object shown in Fig. 2. In Tab. 7, it is shown few complete and reduced signatures of the $\boldsymbol{I_1}$ and $\boldsymbol{I_2}$ contour images. For easy viewing, the corresponding signatures describing the same point in the two images were marked manually with the same color. (Fig. 11).

Table 7. Full and reduced signatures of the range images – Horse Model.

RANGE IMAGE $\boldsymbol{I_1}$		RANGE IMAGE $\boldsymbol{I_2}$	
Full Signature	Reduced Signature	Full Signature	Reduced Signature
31000	31	20123	2123
20123	2123	11223	1123
11223	3023	30023	3023
30023	3023	30003	303
30003	303	30013	3013
30013	313	30023	3023
30023	323	30003	303

The methodology proposed to register range images has two parts: rough alignment and fine alignment. The first part has been discussed and it is the most difficult step. The second part uses the ICP algorithm. This algorithm is referred by many authors concerning image registration. In this article, the ICP will not be discussed in detail, which can be found in (Gerardo Pizo, 2014).

Figure 12 visually presents the registration of a pair of range images. Table 8 displays the variables that contribute to the measurement uncertainty, with the symbol adopted and its probability distribution (ISO GUM, 2008).

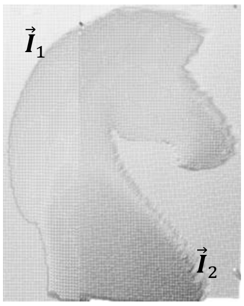

(a).

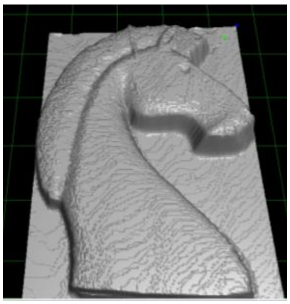

(b).

Table 8. Measurement uncertainty sources – $\boldsymbol{I}_{\text{register}}$

Comp.	Tp	$\bar{x}$	s	ν	PDF	u	$U_{95\%}$ $K=2$
e_R	A	0.89^0	0,061°	15	N	0,00406°	0.00812
e_T	A	1.15 (mm)	0,173 (m m)	15	N	0,01153 (mm)	0.02306

Comp. → Components
Tp. → Function Type
$\bar{x}$ → Average Value
S → Standard Deviation
ν → Degrees of Freedom
PDF → Probability Density Function
U → Standad Uncertainty.
N → Normal Distribution
U → Expanded Uncertainty
e_R → Rotation error
e_T → Translation Error

Figure. 12. Range Image $\boldsymbol{I}_{\text{register}}$ (a) result of the fine alignment using the ICP algorithm in the range image pairs $\boldsymbol{I}_1$ e $\boldsymbol{I}_2$. $e_R = 0.89^0$ and e_T=1.15. (b) Surface representation by using Nurbs patches.

3. CONCLUSIONS

The main problem of the rough alignment is the lack of data to recognize the match between the overlapping regions; for this reason, the most common solution is to choose points that have some characteristic that differs from the rest. Considering the type of surfaces to be treated, it is proposed a methodology that is based on segmentation/reconstruction of range images making use of the technique of edge detection combined with a grouping technique. It was decided to extract the contour curves from the object. The objective was to design a descriptor that detects feature points from the variation of the curvature, which is invariant to similarity transformations (scale, rotation and translation). The search for matches between two point clouds is achieved through signature comparisons. As several feature points must be found, several similarity transformations will be expressed. To check the validity of the transformations, each of them undergo an evaluation of the fitting errors between the two range images through the ICP algorithm. The main contribution of this work is the development of a rough alignment technique and its integration with a fine alignment algorithm, establishing a complete methodology for registration and 3D model reconstruction.

4. REFERENCES

Besl, P and McKay, N., (1992). "A method for registration of 3-D shapes". *IEEE Transaction on Pattern Analysis and Machine Intelligence*. Vol. 14, Issue 2, p.p 239–256.

Chui, K. L., Chiu, W. K. e Yu, K. M. (2008). "Direct 5-Axis Tool-path Generation from Point Cloud Input Using 3D Biarc Fitting." *Robotics and Computer-Integrated Manufacturing. Department of Industrial and Systems Engineering*, Vol.24, Issue 2, pp 270–286.

Ginani, L.S. (2008)., *Desenvolvimento de um Sistema de Digitalização Tridimensional de Superfícies Baseado em Visão Computacional com Varredura a Laser para Uso em Metrologia Dimensional*. Dissertação de Mestrado em Sistemas Mecatrônicos, Publicação ENM.DM-18A/2008, Departamento de Engenharia Mecânica, Universidade de Brasília, Brasília, DF, 187p.

Idrobo-Pizo, G. A., (2009).,*Sistema Computacional para Tratamento de Nuvens de Pontos e Reconstrução Tridimensional de Superfícies Baseada em Modelos Deformáveis*. Dissertação de Mestrado em Sistemas Mecatrônicos, Publicação Agosto/2009, Departamento de Engenharia Mecânica, Universidade de Brasília, Brasília, DF, 126 p.

ISO GUM (2008). *Guide to the expression of uncertainty in measurement - Propagation of distributions using a Monte Carlo method*.Geneve, First edition.

Freeman, H., and Davis, L. S.(1977). "A Corner Finding Algorithm for Chain Coded Curves". In: IEEE Transactions in Computing, Vol. 26, issue 3, pp 297–303.

Planitz, B. M., *et al*., (2005). "The correspondence framework for 3d surface matching algorithms". *Computer Vision and Image Understanding*. Volume 97, Issue 3, Pages 347–383.

Pizo, Gerardo(2014). Projeto de um descritor para o alinhamento de imagens de profundidade de superfícies com aplicação em visão robótica.Tese de Doutorado – Universidade de Brasília. Faculdade de Tecnologia.

5. RESPONSIBILITY NOTICE

The authors are the only responsible for the printed material included in this paper.